

The Gas-Phase H/D Exchange Mechanism of Protonated Amino Acids

Marko Rožman

Laboratory for Chemical Kinetics and Atmospheric Chemistry, Ruđer Bošković Institute, Zagreb, Croatia

A mass spectrometry and Density Functional Theory study of gas-phase H/D exchange in protonated Ala, Cys, Ile, Leu, Met, and Val is reported. Site-specific rate constants were determined and results identify the α -amino group as the protonation site. Lack of exchange on the Cys thiol group is explained by the absence of strong intramolecular hydrogen bonding within the reaction complex. In aliphatic amino acids the presence of a methyl group at the β -C atom was found to lower the site-specific H/D exchange rate for amino hydrogens. Study of the exchange mechanism showed that isotopic exchange occurs in two independent reactions: in one, only the carboxylic hydrogen is exchanged and in the other, both carboxylic and amino group hydrogens exchange. The proposed reaction mechanisms, calculated structures of various species, and a number of structural findings are consistent with experimental data. (J Am Soc Mass Spectrom 2005, 16, 1846–1852) © 2005 American Society for Mass Spectrometry

One of the mass spectrometry techniques capable of going beyond primary structural investigations is gas-phase H/D exchange. Although gas-phase H/D exchange reactions are widely used [1–23], only the reaction mechanism with ND_3 as the deuterating agent has been studied in detail [24]. Several studies discussed simplified mechanisms of H/D exchange reactions with CH_3OD and D_2O as deuterium donors. Gur et al. [7] suggested that H/D exchange in dipeptides occurs through stabilization of a reaction complex [dipeptide – H] – HD_2O^+ . Green and co-workers [2] proposed a schematic mechanism in which H/D exchange begins with formation of a hydrogen bonded complex between a protonated amino acid and a deuteration reagent, Scheme 1.

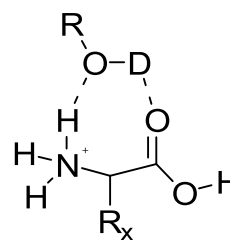
Campbell et al. [6] proposed several H/D exchange mechanisms for different sites of polypeptide molecules. They studied exchange mechanisms by PM3 and AM1 semiempirical calculations where some reaction intermediates were determined and then fitted into the proposed reaction coordinate. For protonated glycine they reported only one exchange, which they assigned to the carboxylic hydrogen. Also, they suggested that carboxylic hydrogen exchange proceeds by either a “salt-bridge” or “flip-flop” mechanism, Scheme 2.

Because of the complex structure of biomolecules, it is difficult to unambiguously interpret H/D exchange results. Therefore, to interpret them correctly, it is important to consider the interaction of the biomolecule with a deuterium donor, the structure of the reaction complex, and the mechanism of isotopic exchange. This

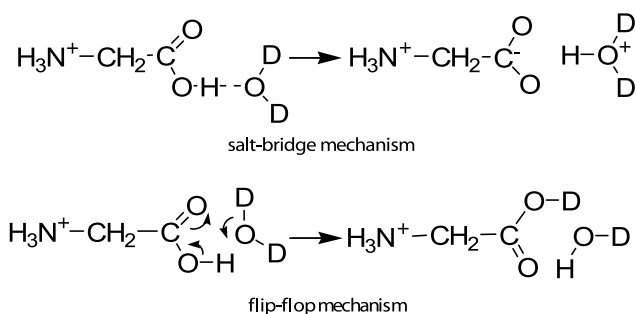
motivated us to investigate thoroughly the gas-phase H/D exchange reactions of protonated amino acids, Ala, Cys, Ile, Leu, Met, and Val with D_2O and CD_3OD . Here, a mass spectrometric investigation of hydrogen bonds in the reaction complex and the effects of the aliphatic side chains, accompanied by the corresponding density functional theory (DFT) description of the dynamic pathway for H/D exchange between AlaH^+ and D_2O , are given and discussed.

Experimental

All amino acids (Ala, Cys, Ile, Leu, Met, and Val) and amino acid methyl esters (AlaOMe, LeuOMe, and ValOMe) were obtained from Fluka (Buchs, Switzerland). The deuteration reagent D_2O (99.8%) was from Aldrich (Milwaukee, WI) and CD_3OD (99.8%) was from Cambridge Isotope Laboratories (Andover, MA). MALDI samples were prepared with a standard dried-droplet procedure using 2,5-dihydroxybenzoic acid (DHB) as the matrix. Two consecutive 337 nm laser pulses from a nitrogen laser (VSL 337 NSD, LSI Laser Science, Newton, MA) were used to produce gas-phase samples. The H/D exchange experiments were performed in a 3 T Fourier transform ion cyclotron resonance (FTICR)



Scheme 1



Scheme 2

mass spectrometer (Extrel FTMS 2001, Madison, WI). The stabilized reagent gas pressure used in the exchange experiments was $2.67\text{--}1.33 \cdot 10^{-5}$ Pa at an ambient temperature of 300 K. The pressure measurement, H/D exchange experiments and determination of the site-specific reaction rate constants were performed by using the procedure described previously [18]. Repetitive H/D exchange experiments indicate a relative standard deviation of up to 30% for the reported site-specific rate constants.

DFT calculations were performed using the Gaussian 03 [25] program package. Although initial checks of the potential energy surface were done using a B3LYP functional with 6-31G* basis set, attempts to identify reaction intermediate **HD3** were unsuccessful. On the other hand, optimization at the B3LYP/6-311++G** level successfully identified minimum **HD3** so all further calculations were done directly with the 6-311++G** basis set. Each stationary point (minimum on the potential energy surface) was tested by a harmonic vibrational analysis. The structures of the transition states were obtained by QST2 and QST3 optimization procedures. Transition-state structures were verified by harmonic frequency analysis and by intrinsic reaction coordinate (IRC) analysis for the reaction pathways. IRC analysis of the reaction pathway from transition-state **TS-HD23** to reaction intermediates **HD2** and **HD3** was unsuccessful. The same analysis (only for **TS-HD23**) was successfully carried out using the GAMESS [26] software package. Energies of reactants and reaction intermediates were not corrected for zero point energies. The basis set superposition error (BSSE) counterpoise corrected potential energy profile for the “flip-flop” mechanism was calculated and it was found that relative energies of conformers vary up to 2

kJ mol^{-1} , so it was assumed that relative energies of studied structures are independent of BSSE. To test if changes of the density functionals alter structures and (or) potential energy surface of the studied reactions, the “flip-flop” reaction mechanism was calculated at the B3PW91/6-311++G** level and found to be in good agreement with B3LYP results (relative energies changed by 3 kJ mol^{-1}).

Results and Discussion

H/D Exchange of Protonated Aliphatic Amino Acids

Compounds selected for this study were: (1) amino acids with aliphatic side chains, e.g., Ala, Ile, Leu, and Val. They were selected because their side chains do not contain active sites that can exchange hydrogen(s) or participate in formation of additional hydrogen bonds within the reaction complex. (2) amino acids Cys and Met with side chains containing sulfur atoms. The absence of gas-phase H/D exchange in reactions of protonated amino acids with D_2S suggests weak hydrogen bonding within the protonated amino acid- D_2S complex [18]. Stabilization through formation of a weakly hydrogen bonded reaction complex with D_2S was not sufficient to overcome the reaction barrier for isotopic exchange. Thus, it was assumed that the CysH^+ thiol group hydrogen would also not be exchanged.

Because all selected amino acids have similar proton affinities [27] and consequently, similar proton affinity differences between amino acid and deuterium donor, one can also expect similar reactivity, i.e., similar H/D reaction rates.

Gas-phase H/D exchange of protonated amino acids and protonated amino acid methyl esters with CD_3OD and D_2O was observed. The studied amino acids exchanged all labile hydrogens but no exchange of CysH^+ thiol group hydrogen was observed, consistent with the assumption above. The reaction data were analyzed and site-specific reaction rate constants were determined (Table 1 and Table 2).

Kinetic results show one fast and three equivalent slow exchanging hydrogens for all amino acids. Results for protonated amino acid methyl esters show three equivalent exchanging hydrogens. By comparison with protonated amino acids, the single nonequivalent fast

Table 1. Site-specific H/D exchange rate constants ($\times 10^{-11} \text{ cm}^3 \text{ s}^{-1} \text{ molecules}^{-1}$) for reaction of the studied protonated amino acids with CD_3OD and D_2O

Amino Acid Deuterium Donor	AlaH^+		CysH^+		IleH^+		LeuH^+		MetH^+		ValH^+	
	CD_3OD	D_2O										
k_1	127	4.44	106	5.16	89.2	1.99	87.4	2.84	78.2	4.05	78.2	2.12
k_2	1.22	0.52	1.38	0.47	0.58	0.39	1.15	0.44	1.01	0.65	0.74	0.31
k_3	1.22	0.52	1.38	0.47	0.58	0.39	1.15	0.44	1.01	0.65	0.74	0.31
k_4	1.22	0.52	1.38	0.47	0.58	0.39	1.15	0.44	1.01	0.65	0.74	0.31

Table 2. Site-specific H/D exchange rate constants ($\times 10^{-11}$ $\text{cm}^3 \text{s}^{-1} \text{molecules}^{-1}$) for reaction of the studied protonated amino acids methyl esters with CD_3OD and D_2O

Methyl ester Deuterium Donor	AlaOMeH ⁺		LeuOMeH ⁺		ValOMeH ⁺	
	CD ₃ OD	D ₂ O	CD ₃ OD	D ₂ O	CD ₃ OD	D ₂ O
k_1	1.61	0.62	0.97	0.6	0.61	0.25
k_2	1.61	0.62	0.97	0.6	0.61	0.25
k_3	1.61	0.62	0.97	0.6	0.61	0.25

exchanging site can be attributed to the carboxylic group. Therefore, three equivalent exchanging sites strongly imply that the amino group is the protonation site, in agreement with theoretical results [28]. Site-specific kinetic studies [9, 13] done on a similar system (glycine) give us an opportunity to compare results. The observation of one fast and three equivalent slow exchanging hydrogens is the same in all studies. Experimental values of the rate constants are consistent with those obtained by Green and Lebrilla [9], while there is some inconsistency in the magnitude (arising mainly from the pressure measurement) with those obtained by He and Marshall [13].

The constants show a surprising decrease in amino group hydrogen exchange rates for IleH⁺ and ValH⁺. Because only IleH⁺ and ValH⁺ have a methyl group at their β -C atoms, a possible steric effect of this methyl group on the most stable conformations of IleH⁺ and LeuH⁺ was analyzed theoretically.

Eight initial structures of both amino acids were built from the structures protonated at the nitrogen with a hydrogen bond between the $-\text{NH}_3^+$ group and the carbonyl oxygen. Aliphatic side chains in both amino acids were placed in various positions with steric strain taken into consideration. Obtained structures were then fully optimized at the B3LYP/6-31G* level to yield five stable structures. The three energetically lowest conformers were subsequently fully optimized at the B3LYP/6-311++G** level to obtain their relative stabilities. The lowest energy conformations of IleH⁺ and LeuH⁺ are shown in Figure 1. The corresponding B3LYP/6-311++G** energies and relative stabilities (Δ) are listed in Table 3.

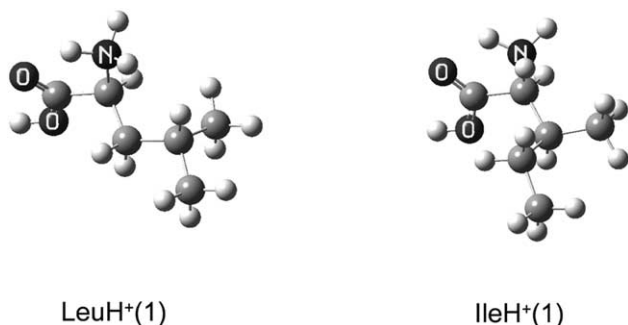


Figure 1. Optimized structures of IleH⁺(1) and LeuH⁺(1) obtained at the B3LYP/6-311++G** level.

Table 3. The B3LYP/6-311++G** energies (in E_h) and relative stabilities (in kJ mol^{-1}) of IleH⁺ and LeuH⁺ conformers

Structure	B3LYP/6-31G*		B3LYP/6-311++G**	
	E	Δ	E	Δ
LeuH ⁺ (1)	-442.049133	0	-442.189218	0
LeuH ⁺ (2)	-442.048184	2.5	-442.188273	2.5
LeuH ⁺ (3)	-442.0476264	3.9	-442.187728	3.9
IleH ⁺ (1)	-442.048556	0.0	-442.188508	0
IleH ⁺ (2)	-442.046757	4.7	-442.186391	5.6
IleH ⁺ (3)	-442.046769	4.7	-442.18625	5.9

Although an increase of the basis set does not alter significantly the relative energies of the conformers, to get a more accurate description all final conformations and energetics were obtained with the 6-311++G** basis set. The lowest energy conformation of LeuH⁺ is a structure LeuH⁺(1) in which methyl groups at the γ -C atom are oriented away from the amino and carboxylic groups and, therefore, do not pose steric hindrance. However, IleH⁺(1), where the methyl and ethyl groups of the β -C atom are closer to the amino and carboxylic groups, appears to be energetically more stable, Table 4.

Based on these structural data, we presume that a methyl group on the β -C atom of an aliphatic amino acid poses significant steric hindrance for the amino and carboxylic groups, which probably causes the decrease in the amino group hydrogen exchange rate. However, such an assumption needs confirmation through a detailed analysis of the H/D exchange mechanism, *vide infra*.

The H/D Exchange Mechanism

For practical reasons (computational time and resources), the computational study of H/D exchange in protonated aliphatic amino acids was carried out for the smallest molecules used in the experiments: AlaH⁺ and D₂O. AlaH⁺ was used as a model compound for all amino acids except for those in which the side-chain group partakes in the H/D exchange process. D₂O and CD₃OD exhibit similar reactivities, and both participate in a single deuterium exchange per reactive encounter [3, 6], so the mechanism may apply for both. In the calculations, the D₂O molecule was simulated by H₂O.

Interaction of MALDI generated AlaH⁺ (expected to be in the most stable conformation [29] and D₂O begins

Table 4. Distances (in Å) between bolded atoms in the IleH⁺ and LeuH⁺ calculated at the B3LYP/6-311++G** level of theory

	IleH ⁺ (1)	LeuH ⁺ (1)
CH ₃ . . . NH ₃	3.08	4.47
CH ₃ . . . CO	4.84	5.82
CH ₃ . . . COH	4.34	5.39
CH ₃ CH ₂ . . . NH ₃	3.07	-
CH ₃ CH ₂ . . . CO	3.78	-
CH ₃ CH ₂ . . . COH	3.51	-

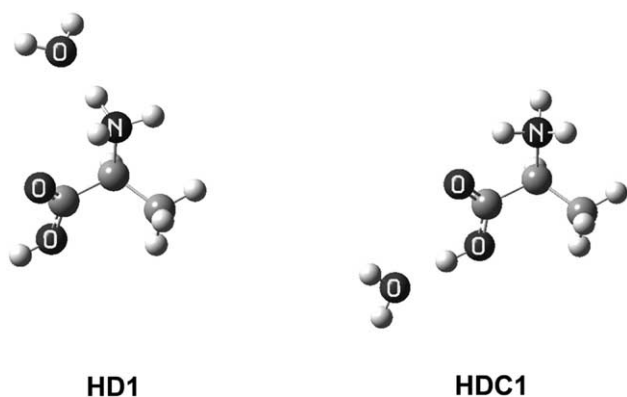


Figure 2. Minima **HD1** and **HDC1**, results of B3LYP/6-311++G** optimization.

with collisions from various directions. Molecular dynamic simulations of interactions in similar systems showed that, depending on the direction, the deuterium donor within a few ps interval stabilizes near the active/preferred site [12, 23]. In AlaH^+ the active sites are the carboxylic and amino groups. Various reaction complexes were generated in such a way that the D_2O molecule was placed in the proximity of the AlaH^+ active sites. The complexes were then optimized at the B3LYP/6-311++G** level (Figure 2). For the carboxylic site, five initial structures gave minimum **HDC1**, while for the amino site, six initial structures gave three

minima (in each minimum molecule D_2O was oriented toward one of the three amino hydrogens, as in **HD1**). **HD1** is a global minimum, however, the energy differences between three amino site minima are very small, less than 2.5 kJ mol^{-1} . Therefore, it is conceivable that during interaction of AlaH^+ and D_2O , D_2O oscillates around the amino group and before isotopic exchange stabilizes into position **HD1**, Figure 2.

The minimum **HD1** is 6.1 kJ mol^{-1} more stable than **HDC1** and therefore we first analyzed the reaction mechanism that originates from **HD1**. The B3LYP/6-311++G** potential energy profile together with optimized structures for the H/D exchange of AlaH^+ with D_2O is shown in Figure 3.

Before describing the reaction mechanism, it is interesting to compare the hydrogen bonded complex proposed by Gard et al. [2] (Scheme 1) with the starting complex **HD1**. In **HD1**, the D_2O molecule is situated (3.14 \AA) away from the carbonyl oxygen without formation of a hydrogen bond between them. Attempts to stabilize the reaction minimum by moving D_2O closer to the oxygen were unsuccessful. A slight move of D_2O towards the carbonyl oxygen is a result of hydroxyl group rotation by 180° around the C–O bond over transition-state **TS-HD12** into **HD2**. Formation of reaction intermediate **HD2** is a prerequisite for the start of isotopic exchange which leads to concerted hydrogen/deuterium transfer from **HD2** in the transition-state **TS-HD23**. Here one of the $-\text{NH}_3^+$ hydrogens is trans-

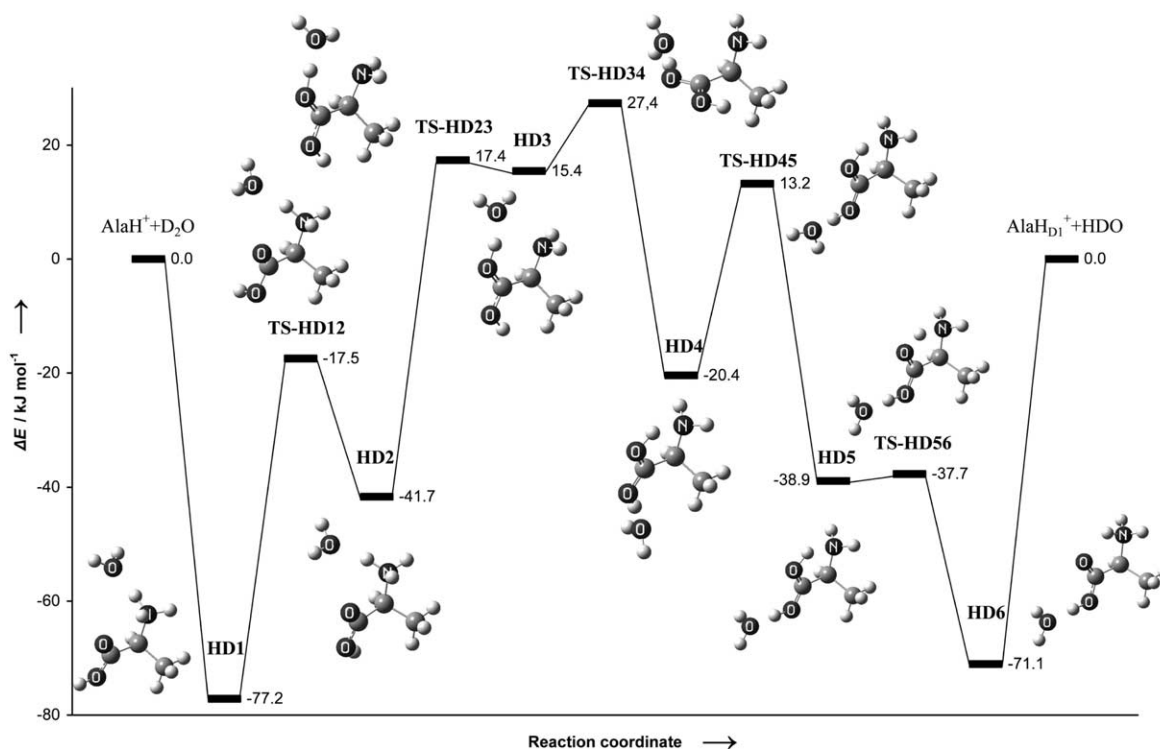


Figure 3. Scheme of the potential energy profile for H/D exchange in AlaH^+ with D_2O . The relative energies and optimized structures were calculated at the B3LYP/6-311++G** level of theory. Also see Table 1 in the Appendix section.

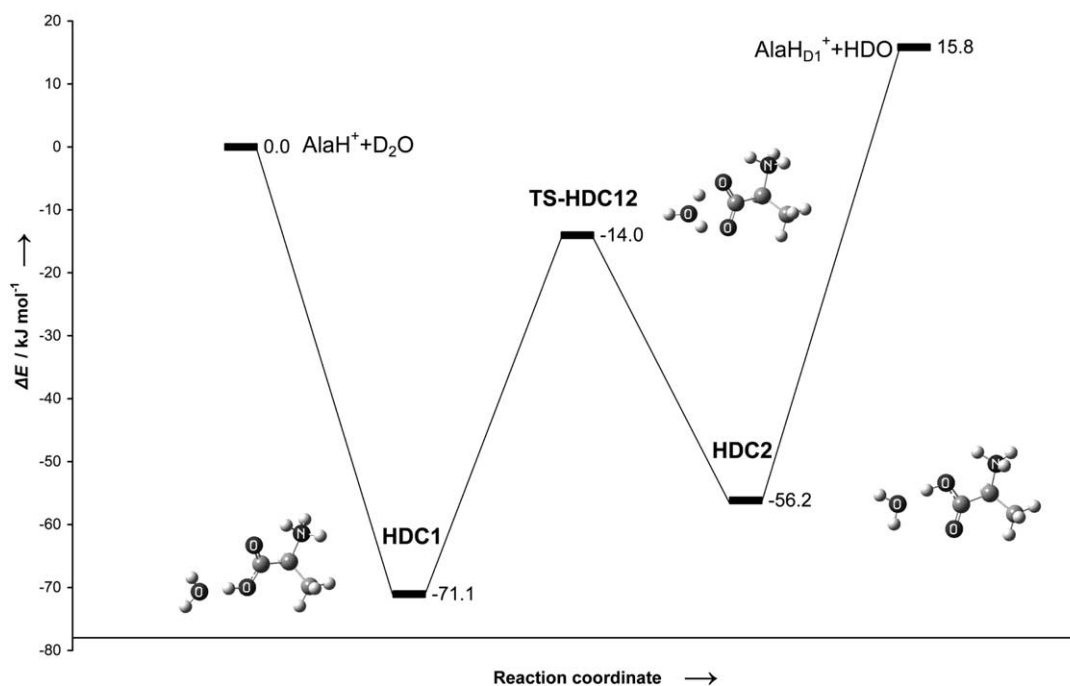


Figure 4. Schematic representation of the potential energy profile for the H/D exchange of the AlaH^+ carboxylic hydrogen with D_2O . The relative energies and optimized structures were calculated at the B3LYP/6-311++G** level of theory. Also see Table 2 in the Appendix section.

ferred to D_2O while, simultaneously, one of the deuteriums moves to the carbonyl oxygen. The imaginary vibrational frequency (48.61 i cm^{-1}) of transition-state **TS-HD23** corresponds to alternate swinging of HDO towards the $-\text{NH}_2$ or $-\text{COD}(\text{OH})$ group of “enolic” AlaH^+ . After the concerted H/D transfer, rotation of the $-\text{COD}(\text{OH})$ group around the C- $\text{C}\alpha$ axis occurs from **HD3** to **HD4**. Simultaneously, the HDO molecule becomes perpendicular to the $-\text{COD}(\text{OH})$ group plane. The corresponding transition-state **TS-HD34** is associated with the energetically highest barrier. The next reaction step is a concerted exothermic rotation of the $-\text{OD}$ group and HDO molecule through the transition-state **TS-HD45** leading to reaction intermediate **HD5**. Finally, reaction intermediate **HD6** with a protonated α -amino group is formed by proton transfer from $-\text{DOCOH}$ to the $-\text{NH}_2$ group from reaction intermediate **HD5**.

The reaction energy profile (Figure 3) shows that the energy gain from initial **HD1** reaction complex formation is not sufficient to overcome the reaction barrier(s) and, consequently, low reaction rates will result. Furthermore, this mechanism gives equal exchange rates for carboxylic and amino hydrogens while experimental results [9, 13, 18] suggest that a carboxylic hydrogen is exchanged 10 to 100 times faster than one of the amino group.

The above findings suggest existence of an additional mechanism for the carboxylic hydrogen exchange. Campell et al. [6] already proposed the “flip-flop” and “salt-bridge” mechanisms for exchange. Present calculations suggest that H/D exchange at the

carboxylic oxygen via proton transfer by formation of a “hydronium” cation is very unfavorable, and our attempts to find this mechanism were unsuccessful. On the other hand, the “flip-flop” mechanism which starts from minimum **HDC1** appears to be essentially barrierless, Figure 4.

The H/D exchange process is described through the transition-state **TS-HDC12**, which represents concerted double hydrogen/deuterium transfer. The energy barrier towards transition-state **TS-HDC12** is overcome by stabilization of the intermediate **HDC1** resulting in fast exchange of the carboxylic hydrogen, consistent with experimental results. Of course, after or during dissociation of **HDC2**, $\text{AlaH}_{\text{D}1}^+$ returns (not shown in Figure 4) to its most stable conformation, which results in needed product stabilization.

It follows that H/D exchange of protonated aliphatic amino acids is the result of two reactions: in the faster and energetically more favorable first reaction, only the carboxylic hydrogen is exchanged while in the second reaction, both carboxylic and amino group hydrogens are exchanged. As experimental support for this model we consider the following: (1) fast exchange of the hydroxylic hydrogen, which is essentially thermo neutral and whose exchange rates are 10 to 100 times faster than those for amino group hydrogens [13, 18], and (2) decrease of the amino group hydrogen exchange rates in IleH^+ and ValH^+ because their additional methyl group on β -C atoms hinders the $-\text{COD}(\text{OH})$ group rotation around the C- $\text{C}\alpha$ axis and slows down the reaction. The opposite behavior, i.e., fast exchange of the amino group hydrogens can be found in H/D

experiments with molecules where the carbonyl group rotation is likely constrained (e.g., GlyGlyH⁺) [17], or where deuterium donor binding could be stabilized by two nitrogen atoms (e.g., HisH⁺) [11].

Conclusions

The results of this study lead to three main conclusions. (1) Gas-phase isotopic exchange of protonated aliphatic amino acids with deuterium donors proceeds by two independent reactions: fast exchange of only the carboxylic hydrogen and slow exchange of both the carboxylic and the amino group hydrogens. (2) The reaction energy barrier for isotopic exchange is overcome by energy gained from formation of the initial multiply hydrogen bonded reaction complex. (3) Steric hindrance from the presence of a methyl group at the β -C atom decreases the site-specific H/D exchange rate of amino group hydrogens.

Acknowledgments

The author gratefully acknowledges helpful discussions with Dr. Dunja Srzić, Dr. Leo Klasinc, and Goran Kovačević. The Ministry of Science, Education, and Sports of Republic of Croatia and Croatian Academy of Sciences and Arts Foundation supported this work.

Appendix

Table 1. (with Figure 3) The B3LYP/6-311++G** energies (in E_h) and relative stabilities of conformers (in kJ mol^{-1}) for H/D exchange in AlaH⁺ with D₂O

Structure	E	Δ
AlaH ⁺ + D ₂ O	-400.670099	0.0
HD1	-400.699490	-77.2
TS-HD12	-400.676754	-17.5
HD2	-400.685966	-41.7
TS-HD23	-400.663487	17.4
HD3	-400.664215	15.4
TS-HD34	-400.659679	27.4
HD4	-400.677887	-20.4
TS-HD45	-400.665061	13.2
HD5	-400.684912	-38.9
TS-HD56	-400.684449	-37.7
HD6	-400.697164	-71.1
AlaH _{D1} ⁺ + HDO	-400.670099	0.0

Table 2. (with Figure 4) The B3LYP/6-311++G** energies (in E_h) and relative stabilities of conformers (in kJ mol^{-1}) for the H/D exchange of AlaH⁺ carboxylic hydrogen with D₂O

Structure	E	Δ
AlaH ⁺ + D ₂ O	-400.670099	0.0
HDC1	-400.697164	-71.1
TS-HDC12	-400.675448	-14.0
HDC2	-400.691495	-56.2
AlaH _{D1} ⁺ + HDO	-400.66407	15.8

References

- Gard, E.; Willard, D.; Bregar, J.; Green, M. K.; Lebrilla, C. B. Site Specificity in the H/D Exchange Reaction of Gas-Phase Protonated Amino Acids with CH₃OD. *Org. Mass Spectrom.* **1993**, *28*, 1632–1639.
- Gard, E.; Green, M. K.; Bregar, J.; Lebrilla, C. B. Gas-Phase Hydrogen/Deuterium Exchange as a Molecular Probe for the Interaction of Methanol and Protonated Peptides. *J. Am. Soc. Mass Spectrom.* **1994**, *5*, 623–631.
- Campbell, S.; Rodgers, M. T.; Marzluff, E. M.; Beauchamp, J. L. Structural and Energetic Constraints on Gas-Phase Hydrogen/Deuterium Exchange Reactions of Protonated Peptides with D₂O, CD₃OD, CD₃CO₂D, and ND₃. *J. Am. Chem. Soc.* **1994**, *116*, 9765–9766.
- Green, M. K.; Gard, E.; Bregar, J.; Lebrilla, C. B. H-D Exchange Kinetics of Alcohols and Protonated Peptides: Effects of Structure and Proton Affinity. *J. Mass Spectrom.* **1995**, *30*, 1103–1110.
- Wu, J.; Gard, E.; Bregar, J.; Green, M. K.; Lebrilla, C. B. Studies of Nearest-Neighbor Interactions Between Amino Acids in Gas-Phase Protonated Peptides. *J. Am. Chem. Soc.* **1995**, *117*, 9900–9905.
- Campbell, S.; Rodgers, M. T.; Marzluff, E. M.; Beauchamp, J. L. Deuterium Exchange as Probe of Biomolecule Structure. Fundamental Studies of Gas-Phase H/D Exchange Reactions of Protonated Glycine Oligomers with D₂O, CD₃OD, CD₃CO₂D, and ND₃. *J. Am. Chem. Soc.* **1995**, *117*, 12840–12854.
- Gur, E. H.; de Koning, L. J.; Nibbering, N. M. M. The Bimolecular Hydrogen-Deuterium Exchange Behavior of Protonated Alkyl Dipeptides in the Gas Phase. *J. Am. Soc. Mass Spectrom.* **1995**, *5*, 466–477.
- Kaltashov, I. A.; Doroshenko, V. M.; Cotter, R. J. Gas Phase Hydrogen/Deuterium Exchange Reactions of Peptide Ions in a Quadrupole Ion Trap Mass Spectrometer. *Proteins: Struct. Funct. Genet.* **1997**, *28*, 53–58.
- Green, M. K.; Lebrilla, C. B. Ion-Molecule Reactions as Probes of Gas-Phase Structures of Peptides and Proteins. *Mass Spectrom. Rev.* **1997**, *16*, 53–71.
- Freitas, M. A.; Hendrickson, C. L.; Emmett, M. R.; Marshall, A. G. High-Field Fourier Transform Ion Cyclotron Resonance Mass Spectrometry for Simultaneous Trapping and Gas-Phase Hydrogen/Deuterium Exchange of Peptide Ions. *J. Am. Soc. Mass Spectrom.* **1998**, *9*, 1012–1019.
- Green, M. K.; Lebrilla, C. B. The Role of Proton-Bridged Intermediates in Promoting Hydrogen-Deuterium Exchange in Gas-Phase Protonated Diamines, Peptides and Proteins. *Int. J. Mass Spectrom. Ion Processes* **1998**, *175*, 15–26.
- Wytenbach, T.; Bowers, M. T. Gas Phase Conformations of Biological Molecules: The Hydrogen/Deuterium Exchange Mechanism. *J. Am. Soc. Mass Spectrom.* **1999**, *10*, 9–14.
- He, F.; Marshall, A. G. Weighted Quasi-Newton and Variable-Order, Variable-Step Adams Algorithm for Determining Site-Specific Reaction Rate Constants. *J. Phys. Chem. A* **2000**, *104*, 562–567.
- Schaaff, T. G.; Stephenson, J. L., Jr.; McLuckey, S. A. Gas Phase H/D Exchange Kinetics: DI versus D₂O. *J. Am. Soc. Mass Spectrom.* **2000**, *11*, 167–171.
- Hofstadler, S. A.; Sannes-Lowery, K. A.; Griffey, R. H. Enhanced Gas-Phase Hydrogen-Deuterium Exchange of Oligonucleotide and Protein Ions Stored in an External Multipole Ion Reservoir. *J. Mass Spectrom.* **2000**, *35*, 62–70.
- Reyzer, M. L.; Brodbelt, J. S. Gas-Phase H/D Exchange Reactions of Polyamine Complexes: (M + H)⁺, (M + alkali metal)⁺, and (M + 2H)²⁺. *J. Am. Soc. Mass Spectrom.* **2000**, *11*, 711–721.
- He, F.; Marshall, A. G.; Freitas, M. A. Assignment of Gas-Phase Dipeptide Amide Hydrogen Exchange Rate Constants

- by Site-Specific Substitution: GlyGly. *J. Phys. Chem. B* **2001**, *105*, 2244–2249.
18. Rožman, M.; Kazazić, S.; Klasinc, L.; Srzić, D. Kinetic of Gas-Phase Hydrogen/Deuterium Exchange and Gas-Phase Structure of Protonated Phenylalanine, Proline, Tyrosine and Tryptophan. *Rapid Commun. Mass Spectrom.* **2003**, *17*, 2769–2772.
 19. Evans, S. E.; Lueck, N.; Marzluff, E. M. Gas Phase Hydrogen/Deuterium Exchange of Proteins in an Ion Trap Mass Spectrometer. *Int. J. Mass Spectrom.* **2003**, *222*, 175–187.
 20. Reuben, B. G.; Ritov, Y.; Geller, O.; Mc Farland, M. A.; Marshall, A. G.; Lifshitz, C. Applying a New Algorithm for Obtaining Site Specific Rate Constants for H/D Exchange of the Gas Phase Proton-Bound Arginine Dimer. *Chem. Phys. Lett.* **2003**, *380*, 88–94.
 21. Lifshitz, C. A review of gas-phase H/D exchange experiments: the protonated arginine dimer and bradykinin nonapeptide systems. *Int. J. Mass Spectrom.* **2004**, *234*, 63–70.
 22. Cox, H. A.; Julian, R. R.; Lee, S. W.; Beauchamp, J. L. Gas-Phase H/D Exchange of Sodiated Glycine Oligomers with ND₃: Exchange Kinetics Do Not Reflect Parent Ion Structures. *J. Am. Chem. Soc.* **2004**, *126*, 6485–6490.
 23. Rožman, M.; Bertoša, B.; Klasinc, L.; Srzić, D. Gas Phase H/D Exchange of Sodiated Amino Acids: Why Do We See Zwitterions? Unpublished.
 24. Balata, B.; Basma, M.; Aviyente, V.; Zhu, C.; Lifshitz, C. Structures and Reactivity of Gaseous Glycine and its Derivatives. *Int. J. Mass Spectrom.* **2000**, *201*, 69–85.
 25. M. J.; Frisch, G. W.; Trucks, H. B.; Schlegel, G. E.; Scuseria, M. A.; Robb, J. R.; Cheeseman, J. A.; Montgomery, Jr., T.; Vreven, K. N.; Kudin, J. C.; Burant, J. M.; Millam, S. S.; Iyengar, J.; Tomasi, V.; Barone, B.; Mennucci, M.; Cossi, G.; Scalmani, N.; Rega, G. A.; Petersson, H.; Nakatsuji, M.; Hada, M.; Ehara, K.; Toyota, R.; Fukuda, J.; Hasegawa, M.; Ishida, T.; Nakajima, Y.; Honda, O.; Kitao, H.; Nakai, M.; Klene, X.; Li, J. E.; Knox, H. P.; Hratchian, J. B.; Cross, C.; Adamo, J.; Jaramillo, R.; Gomperts, R. E.; Stratmann, O.; Yazyev, A. J.; Austin, R.; Cammi, C.; Pomelli, J. W.; Ochterski, P. Y.; Ayala, K.; Morokuma, G. A.; Voth, P.; Salvador, J. J.; Dannenberg, V. G.; Zakrzewski, S.; Dapprich, A. D.; Daniels, M. C.; Strain, O.; Farkas, D. K.; Malick, A. D.; Rabuck, K.; Raghavachari, J. B.; Foresman, J. V.; Ortiz, Q.; Cui, A. G.; Baboul, S.; Clifford, J.; Cioslowski, B. B.; Stefanov, G.; Liu, A.; Liashenko, P.; Piskorz, I.; Komaromi, R. L.; Martin, D. J.; Fox, T.; Keith, M. A.; Al-Laham, C. Y.; Peng, A.; Nanayakkara, M.; Challacombe, P. M. W.; Gill, B.; Johnson, W.; Chen, M. W.; Wong, C.; Gonzalez, J. A. Pople, Gaussian 03, Revision B. 05; Gaussian, Inc.: Pittsburgh, PA, 2003.
 26. Schmidt, W.; Baldrige, K. K.; Boatz, J. A.; Elbert, S. T.; Gordon, S.; Jensen, J. H.; Koseki, S.; Matsunaga, N.; Nguyen, K. A.; Su, S. J.; Windus, T. L.; Dupuis, M.; Montgomery, J. A. General Atomic and Molecular Electronic Structure System. *J. Comput. Chem.* **1993**, *14*, 1347–1363.
 27. Hunter, E. P.; Lias, S. G. Evaluated Gas Phase Basicities and Proton Affinities of Molecules. (NIST Chemistry WebBook). *J. Phys. Chem. Ref. Data* **1998**, *27*, 413–656.
 28. Noguera, M.; Rodriguez-Santiago, L.; Sodupe, M.; Bertran, J. Protonation of Glycine, Serine, and Cysteine. Conformations, Proton Affinities, and Intrinsic Basicities. *J. Mol. Struct. Theoret. Chem.* **2001**, *537*, 307–318.
 29. Karas, M.; Glückmann, M.; Schäfer, J. Ionization in Matrix-Assisted Laser Desorption/Ionization: Singly Charged Molecular Ions are the Lucky Survivors. *J. Mass Spectrom.* **2000**, *35*, 1–12.